
Provably Robust Cost-Sensitive Learning via Randomized Smoothing

Yuan Xin Michael Backes Xiao Zhang

CISPA Helmholtz Center for Information Security
Saarbrücken, Germany

{yuan.xin, backes, xiao.zhang}@cispa.de

Abstract

We study the problem of robust learning against adversarial perturbations under cost-sensitive scenarios, where the potential harm of different types of misclassifications is encoded in a cost matrix. Existing approaches are either empirical and cannot certify robustness or suffer from inherent scalability issues. In this work, we investigate whether randomized smoothing, a scalable framework for robustness certification, can be leveraged to certify and train for cost-sensitive robustness. Built upon the notion of cost-sensitive certified radius, we first illustrate how to adapt the standard certification algorithm of randomized smoothing to produce tight robustness certificates for any binary cost matrix, and then develop a robust training method to promote certified cost-sensitive robustness while maintaining the model’s overall accuracy. Through extensive experiments on image benchmarks, we demonstrate the superiority of our proposed certification algorithm and training method under various cost-sensitive scenarios. Our implementation is available as open source code at: <https://github.com/TrustMLRG/CS-RS>.

1 Introduction

Recent studies have revealed that deep neural networks are highly vulnerable to classifying adversarial examples (Szegedy et al., 2013; Goodfellow et al., 2014). To improve model robustness against adversarial perturbations, numerous defensive mechanisms have been proposed, which primarily fall into two categories: empirical defenses (Goodfellow et al., 2014; Papernot et al., 2016; Kurakin et al., 2016; Madry et al., 2017; Zhang et al., 2019; Carmon et al., 2019) and certifiable methods (Raghunathan et al., 2018; Wong & Kolter, 2018; Gowal et al., 2018; Cohen et al., 2019; Lecuyer et al., 2019; Jia et al., 2019; Li et al., 2019). Compared with empirical defenses, certifiable methods can produce a robustness certificate for the model prediction to remain unchanged within some specific norm-bounded perturbation ball of any test input, and train models to be provably robust with respect to the derived certificate. These methods avoid the undesirable arms race between empirical defenses that claim robustness against existing attacks and newly devised adaptive attacks that can further break them (Carlini & Wagner, 2017; Athalye et al., 2018).

Most existing defenses are designed to improve overall model robustness, assuming the same penalty on all kinds of adversarial misclassifications. For real-world applications, however, it is likely that certain type of misclassifications are more consequential than others (Domingos, 1999; Elkan, 2001). For instance, misclassifying a malignant tumor as benign in the application of medical diagnosis is much more detrimental to a patient than the reverse. Therefore, instead of solely focusing on overall robustness, the development of defenses should account for the difference in costs induced by different adversarial examples. In line with existing works on cost-sensitive robust learning (Domingos, 1999; Asif et al., 2015; Zhang & Evans, 2019; Chen et al., 2021), we aim to develop models that are robust to cost-sensitive adversarial misclassifications, while maintaining the standard overall classification

accuracy. Nevertheless, previous methods for promoting cost-sensitive robustness (Domingos, 1999; Asif et al., 2015; Chen et al., 2021; Zhang & Evans, 2019) are either hindered by their foundational reliance on heuristics, which often fall short of providing a robustness guarantee or suffer from inherent scalability issues when certifying robustness for large models and perturbations.

To achieve the best of both worlds, we propose to learn provably cost-sensitive robust classifiers by leveraging randomized smoothing (Liu et al., 2018; Cohen et al., 2019; Salman et al., 2019), an emerging robustness certification framework that has attracted a lot of attention due to its generality and scalability. However, the standard randomized smoothing techniques are not optimal for certifying cost-sensitive robustness, since they rely on strong assumptions of the smoothed classifier’s predictions, which will largely be violated under cost-sensitive settings. Thus, deriving a tighter, if not the tightest, robustness certification scheme that works for general cost-sensitive settings remains a challenging task. Besides, most existing robust training methods only focus on optimizing overall performance. For cost-sensitive robustness, however, the diverse designs of cost matrices necessitate a more flexible optimization approach, and the multiple available randomized smoothing-based training methods require a systematic study of their suitability for cost-sensitive scenarios.

Contributions. To the best of our knowledge, we are the first to adapt the randomized smoothing framework to certify and train for cost-sensitive robustness. We introduce a notion of *cost-sensitive certified radius* (Definition 3.1), which captures the maximum allowable ℓ_2 perturbation with respect to the smoothed classifier for each sensitive seed input. Built upon this notion, we then develop an empirical certification algorithm using Monte Carlo samples (Algorithm 1), which presents two different approaches to ensure the algorithm always returns a tight robustness certificate under cost-sensitive settings (Theorem 3.3). We explain why the standard certification technique does not apply and highlight the advantages of our algorithm in deriving a general, statistically sound and tight certificate for cost-sensitive robustness (Remark 3.4 and Remark 3.5). In addition, inspired by the design insight of MACER (Zhai et al., 2020), we propose a cost-sensitive robust training method by directly optimizing the certified radius with respect to the smoothed classifier and different data subgroups (Section 4). To illustrate our method’s superiority and ensure a fair comparison, we adapt reweighting schemes from standard literature (Elkan, 2001; Khan et al., 2017) to train cost-sensitive robust classifiers as the baseline methods. Comprehensive experiments on image benchmarks and a real-world medical image dataset demonstrate that our method significantly improves certified cost-sensitive robustness across various cost matrices while maintaining overall accuracy (Section 5).

Related Work. Cohen et al. (2019) proposed the randomized smoothing framework, which first converts any base classifier into a smoothed classifier by injecting Gaussian noises to inputs followed by majority voting, then derives a probabilistic robustness certificate that can guarantee the prediction of the resulting smoothed classifier is constant within some ℓ_2 -norm ball for any given input. Compared with relaxation-based certification methods (Wong & Kolter, 2018; Goyal et al., 2018), the biggest advantage of randomized smoothing is its scalability to deep neural networks and large-scale datasets. SmoothAdv adapts the idea of adversarial training to learn smoothed classifiers with improved robustness (Salman et al., 2019), while MACER directly optimizes the certified radius of a smoothed classifier with respect to correctly classified samples using margin-based loss (Zhai et al., 2020). More recently, research studies (Carlini et al., 2022; Xiao et al., 2022; Zhang et al., 2023) proposed methods to train a better base classifier by leveraging pre-trained diffusion models to denoise samples augmented with Gaussian noise, which attains state-of-the-art certified robustness. Nevertheless, the reverse process of diffusion models required by these methods costs a significant amount of time, posing computational challenges for both training and inference time. In contrast to the aforementioned works, we focus on learning robust classification models with provable certification guarantees under cost-sensitive scenarios. We are aware that Zhang & Evans (2019) also considers a similar cost-sensitive robustness problem to ours. However, their method suffers from inherent scalability issues, especially when certifying deep networks under large perturbations (See Appendix C for empirical evidence and more discussions).

Notation. We use lowercase boldfaced letters to denote vectors and use uppercase boldfaced letters for matrices. Let $[m]$ be the index set $\{1, 2, \dots, m\}$, $|\mathcal{S}|$ be the cardinality of a set \mathcal{S} and $\mathbb{1}(\cdot)$ be the indicator function. For any $\mathbf{x} \in \mathbb{R}^d$ and $i \in [d]$, the i -th element of \mathbf{x} is denoted as x_i . Denote by $\mathcal{N}(\boldsymbol{\mu}, \sigma^2 \mathbf{I})$ the multivariate spherical Gaussian distribution with mean $\boldsymbol{\mu}$ and covariance matrix $\sigma^2 \mathbf{I}$ with $\sigma > 0$. Let $\Phi(\cdot)$ be the CDF of $\mathcal{N}(0, 1)$ and $\Phi^{-1}(\cdot)$ be its inverse.

2 Preliminaries

Randomized Smoothing. Randomized smoothing is a probabilistic certification framework proposed in Cohen et al. (2019). In particular, it builds upon the following definition of smoothed classifiers:

Definition 2.1. Let $\mathcal{X} \subseteq \mathbb{R}^d$ be the input space and $[m]$ be the label space. For any classifier $f_\theta : \mathcal{X} \rightarrow [m]$ and $\sigma > 0$, the *smoothed classifier* with respect to f_θ and σ is defined as:

$$g_\theta(\mathbf{x}) = \arg \max_{k \in [m]} \mathbb{P}_{\delta \sim \mathcal{N}(\mathbf{0}, \sigma^2 \mathbf{I})} [f_\theta(\mathbf{x} + \delta) = k], \forall \mathbf{x} \in \mathcal{X}.$$

Let $h_\theta : \mathcal{X} \rightarrow [0, 1]^m$ be the function that maps any $\mathbf{x} \in \mathcal{X}$ to the prediction probabilities of $g_\theta(\mathbf{x})$:

$$[h_\theta(\mathbf{x})]_k = \mathbb{P}_{\delta \sim \mathcal{N}(\mathbf{0}, \sigma^2 \mathbf{I})} [f_\theta(\mathbf{x} + \delta) = k], \forall k \in [m]. \quad (1)$$

The following lemma, proven in Cohen et al. (2019), characterizes the ℓ_2 perturbation ball with the largest radius for any input \mathbf{x} such that the prediction of g_θ remains the same.

Lemma 2.2 (Cohen et al. (2019)). Let $\mathbf{x} \in \mathcal{X}$ and $y \in [m]$ be its ground-truth label. Suppose g_θ classifies \mathbf{x} correctly, i.e., $y = \arg \max_{k \in [m]} \mathbb{P}_{\delta \sim \mathcal{N}(\mathbf{0}, \sigma^2 \mathbf{I})} [f_\theta(\mathbf{x} + \delta) = k]$, then g_θ is provably robust at \mathbf{x} in ℓ_2 -norm with certified radius $r(\mathbf{x}; h_\theta)$ defined by:

$$r(\mathbf{x}; h_\theta) = \frac{\sigma}{2} \left[\Phi^{-1}([h_\theta(\mathbf{x})]_y) - \Phi^{-1}\left(\max_{k \neq y} [h_\theta(\mathbf{x})]_k\right) \right],$$

where h_θ is defined by Equation 1. When h_θ is free of context, we simply write $r(\mathbf{x}) = r(\mathbf{x}; h_\theta)$.

Cost-Sensitive Robustness. We consider robust classification tasks under cost-sensitive scenarios, where the goal is to learn a classifier with high cost-sensitive robustness while maintaining a similar performance level of overall accuracy. Let $\mathbf{C} \in \{0, 1\}^{m \times m}$ be a predefined cost matrix that encodes the potential harm of different classwise adversarial transformations. For any $j \in [m]$ and $k \in [m]$, $C_{jk} = 1$ means that any misclassification from seed class j to target class k will induce a cost, whereas $C_{jk} = 0$ suggests that there is no incentive for an attacker to trick the model to misclassify inputs from class j to class k . Note that overall robustness corresponds to the cost matrix, where all the entries are 1 except for the diagonal ones. Therefore, the goal of cost-sensitive robust learning can be understood as reducing the number of adversarial misclassifications that will induce a cost defined by \mathbf{C} . For ease of presentation, we introduce the following notations. For any seed class $j \in [m]$, we let $\Omega_j = \{k \in [m] : C_{jk} = 1\}$ be the set of cost-sensitive target classes. If Ω_j is an empty set, then all the examples from seed class j are non-sensitive. Otherwise, any class j with $|\Omega_j| \geq 1$ is a sensitive seed class. Given a dataset $\mathcal{S} = \{(\mathbf{x}_i, y_i)\}_{i \in [n]}$, we define the set of cost-sensitive seed examples as $\mathcal{S}^s = \{(\mathbf{x}, y) \in \mathcal{S} : |\Omega_y| \geq 1\}$, while the remaining examples are regarded as non-sensitive. In this work, we consider the following two categories of cost matrices depending on the cost-sensitive target classes Ω_y : (a) *Seedwise*: For any $(\mathbf{x}, y) \in \mathcal{S}^s$, $\Omega_y = \{j \in [m] : j \neq y\}$ or equivalently $|\Omega_y| = m - 1$, meaning that any possible classwise adversarial transformation for (\mathbf{x}, y) will incur a cost. In other words, Ω_y contains all the possible target classes with respect to (\mathbf{x}, y) , and (b) *Pairwise*: For any $(\mathbf{x}, y) \in \mathcal{S}^s$, $\Omega_y \subsetneq \{j \in [m] : j \neq y\}$, indicating that $[m] \setminus \Omega_y$ includes target class other than y and misclassification to any target class in $[m] \setminus \Omega_y$ is acceptable.

3 Certifying Cost-Sensitive Robustness

3.1 Cost-Sensitive Certified Radius

According to the problem setting of cost-sensitive robustness introduced in Section 2, only misclassifying \mathbf{x} to a target class in Ω_y incurs a cost for any $(\mathbf{x}, y) \in \mathcal{S}^s$. Similar to the standard certified radius in Lemma 2.2, we introduce the definition of *cost-sensitive certified radius* as follows:

Definition 3.1 (Cost-Sensitive Certified Radius). Let \mathbf{C} be an $m \times m$ cost matrix. For any $(\mathbf{x}, y) \in \mathcal{X} \times [m]$ where y is a sensitive seed class, the *cost-sensitive certified radius* at (\mathbf{x}, y) with respect to the smoothed classifier g_θ and the cost matrix \mathbf{C} is defined as:

$$r_{c-s}(\mathbf{x}; \Omega_y, h_\theta) = \frac{\sigma}{2} \left[\Phi^{-1}\left(\max_{k \in [m]} [h_\theta(\mathbf{x})]_k\right) - \Phi^{-1}\left(\max_{k \in \Omega_y} [h_\theta(\mathbf{x})]_k\right) \right],$$

where $\Omega_y = \{k \in [m] : C_{yk} = 1\}$ denotes the set of sensitive target classes and h_θ is defined in Equation 1. When h_θ is free of context, we write $r_{c-s}(\mathbf{x}; \Omega_y) = r_{c-s}(\mathbf{x}; \Omega_y, h_\theta)$.

Based on similar proof techniques of Lemma 2.2 (Cohen et al., 2019), we can show that g_θ is provably robust at \mathbf{x} with certified radius $r_{c-s}(\mathbf{x}; \Omega_y)$ in ℓ_2 norm as long as $g_\theta(\mathbf{x})$ does not incur a cost. Note that the standard $r(\mathbf{x})$ can also serve as a valid certificate under cost-sensitive settings, which is equivalent to $r_{c-s}(\mathbf{x}; \Omega_y)$ under seedwise cost matrix scenarios. The following theorem characterizes the connection between cost-sensitive and standard certified radii under different settings.

Theorem 3.2. Under the same setting of Definition 3.1 and suppose $\arg \max_{k \in [m]} [h_\theta(\mathbf{x})]_k \notin \Omega_y$, then $r_{c-s}(\mathbf{x}; \Omega_y) \geq r(\mathbf{x})$, where the equality holds when $\Omega_y = \{k \in [m] : k \neq y\}$.

The main distinction between $r_{c-s}(\mathbf{x}; \Omega_y)$ and the standard certified radius $r(\mathbf{x})$ lies in the scenario where $|\Omega_y| < m - 1$. The detailed proof of Theorem 3.2 is provided in Appendix A.1. We remark that the advantage of using cost-sensitive certified radius for certification is expected to be more pronounced for (\mathbf{x}, y) with a smaller $|\Omega_y|$, since Φ^{-1} is monotonically increasing and the gap between $\max_{k \neq y} [h_\theta(\mathbf{x})]_k$ and $\max_{k \in \Omega_y} [h_\theta(\mathbf{x})]_k$ is likely to be larger when the size of Ω_y is small (see Figures 2(a) and 2(b) in Section 5.2 for more empirical evidence supporting this argument).

3.2 Proposed Certification Algorithm

Note that the exact computation of the cost-sensitive certified radius requires an infinite number of Gaussian samples, which is not feasible in practice. Following Cohen et al. (2019), we thus resort to Monto Carlo methods to obtain empirical estimates of the certified radius. To ensure both statistical rigorousness and tightness, we propose a novel certification algorithm for certifying cost-sensitive robustness using empirical samples. The pseudocode of our algorithm is depicted in Algorithm 1.

More specifically, our algorithm provides two different ways to compute the $1 - \alpha$ confidence bound for cost-sensitive certified radius $r_{c-s}(\mathbf{x}; \Omega_y)$. The first approach is based on \hat{r}_{std} , which is computed using a level $1 - \alpha$ lower confidence bound on the ground-truth probability of the top class within all classes $[m]$, same as the bound for standard radius used in Cohen et al. (2019) for certifying overall robustness. Note that according to Definition 3.1, the standard certified radius is guaranteed to be less than or equal to the corresponding cost-sensitive certified radius, suggesting that \hat{r}_{std} also serves as a valid $1 - \alpha$ confidence bound for cost-sensitive radius. On the other hand, \hat{r}_{c-s} is computed using both a level $1 - \alpha/2$ lower confidence bound of p_A and a level $1 - \alpha/(2|\Omega_y|)$ upper confidence bound of p_B , the ground-truth probability of the top class in Ω_y . To produce a robustness certificate as tight as possible for any binary cost matrix, the maximum of \hat{r}_{std} and \hat{r}_{c-s} is finally returned, where both \hat{r}_{std} and \hat{r}_{c-s} are guaranteed to be a $1 - \alpha$ confidence lower bound on $r_{c-s}(\mathbf{x}; \Omega_y)$.

The following theorem, proven in Appendix A.2 by union bound, shows the validity of the estimate \hat{r}_{c-s} as a $1 - \alpha$ confidence bound on the certified cost-sensitive radius

Theorem 3.3. For any example (\mathbf{x}, y) and binary cost matrix \mathbf{C} , \hat{r}_{c-s} is a certified cost-sensitive robust radius with at least $1 - \alpha$ confidence over the randomness of Gaussian sampling.

Remark 3.4. Compared with the derivation of statistical bounds for standard certified radius, a key technical contribution of our algorithm is the design of how to compute the upper confidence bound $\overline{p_B}$ over any set of cost-sensitive target classes Ω_y . Recall that the practical certification algorithm in Cohen et al. (2019) directly sets $\overline{p_B} = 1 - \underline{p_A}$ based on simplicity considerations and empirical observations that the ground-truth class probabilities $h_\theta(\mathbf{x})$ not allocated to the top prediction class are mostly entirely allocated to one runner-up class. However, simply setting $\overline{p_B} = 1 - \underline{p_A}$ does not work for certifying cost-sensitive robustness, since the top class in Ω_y is not equivalent to the runner-up class in $[m]$ for many scenarios, leading to a loose certificate of cost-sensitive robustness. Therefore, we provide an alternative procedure for deriving the confidence upper bound on p_B , defined as the maximum class probability over all cost-sensitive target class set Ω_y , by union bounds and carefully setting the confidence levels to ensure a tighter bound (Line 7 of Algorithm 1). To the best of our knowledge, this procedure and its proof are new to the existing literature on randomized smoothing, and particularly important for ensuring a tight certificate for cost-sensitive robustness.

Remark 3.5. Another important feature of the proposed certification algorithm for cost-sensitive robustness is the use of the maximum over \hat{r}_{std} and \hat{r}_{c-s} , which ensures the best possible bound is returned for any example and cost matrix. The gap between \hat{r}_{std} and \hat{r}_{c-s} depends on input-dependent variables such as top class and runner-up class probabilities and hyperparameters such as n and α . Note that there exists scenarios where $\hat{r}_{std} > \hat{r}_{c-s}$. Consider the typical case where the class probabilities $h_\theta(\mathbf{x})$ are mostly allocated to the top class and the runner-up class in $[m]$. Suppose the set of cost-sensitive target classes Ω_y contains the runner-up class, then $\hat{r}_{std} > \hat{r}_{c-s}$ is expected, due to

Algorithm 1 Tight Certification for Cost-Sensitive Robustness

```
1: function CERTIFY( $f_\theta, \sigma, \mathbf{x}, n_0, n, \alpha, \Omega_y$ ) :
2:   count0  $\leftarrow$  SAMPLEUNDERNOISE( $f_\theta, \mathbf{x}, n_0, \sigma$ )
3:    $\hat{c}_A \leftarrow$  top index in count0
4:   count  $\leftarrow$  SAMPLEUNDERNOISE( $f_\theta, \mathbf{x}, n, \sigma$ )
5:    $\hat{r}_{\text{std}} = \Phi^{-1}(\text{LOWERCONFBOUND}(\text{count}[\hat{c}_A], n, 1 - \alpha)) \cdot \sigma$ 
6:    $\underline{p}_A \leftarrow \text{LOWERCONFBOUND}(\text{count}[\hat{c}_A], n, 1 - \frac{\alpha}{2})$ 
7:    $\overline{p}_B \leftarrow \max\{\text{UPPERCONFBOUND}(\text{count}[k], n, 1 - \frac{\alpha}{2|\Omega_y|}) : k \in \Omega_y\}$ 
8:    $\hat{r}_{\text{c-s}} = (\Phi^{-1}(\underline{p}_A) - \Phi^{-1}(\overline{p}_B)) \cdot \sigma/2$ 
9:   if  $\max(\hat{r}_{\text{std}}, \hat{r}_{\text{c-s}}) > 0$  then
10:    return  $\hat{c}_A$  and  $\max(\hat{r}_{\text{std}}, \hat{r}_{\text{c-s}})$ 
11:  else
12:    return ABSTAIN
```

the union $1 - \alpha$ lower confidence bound on both \hat{r}_{std} and $\hat{r}_{\text{c-s}}$ and the monotonicity of inverse CDF function of standard Gaussian Φ^{-1} (See Table 8 in Appendix D.3 for empirical results of $\hat{r}_{\text{std}} > \hat{r}_{\text{c-s}}$).

4 Training for Cost-Sensitive Robustness

In this section, we propose a certified robust training method to achieve an optimal trade-off between cost-sensitive robustness and overall accuracy, which is inspired by the design insight of MACER (Zhai et al., 2020). Among different certified robust training methods, MACER stands out for the pursuit of provably robust cost-sensitive learning because of the following two reasons: (a) it is an attack-free certifiable defense, which eliminates the need for designing specific adversarial attacks for different cost matrices, and (b) it can easily integrate the robust certified radius into the cost-sensitive scheme to directly optimize the trade-off between different data subgroups.

Before introducing our training objective, we first introduce a general class of margin losses. Let $l \leq u$ denote the thresholding parameters. For any $v \in \mathbb{R}$, let $\mathcal{L}_M(v; l, u) = \max\{u - v, 0\} \cdot \mathbb{1}(l \leq v \leq u)$. Here, the indicator function selects data points whose certified radius falls into the range of $[l, u]$. For seedwise cost matrices, the training objective of our method is defined as:

$$\min_{\theta \in \Theta} \left\{ \underbrace{\mathbb{E}_{(\mathbf{x}, y) \sim \mathcal{D}} L_{\text{CE}}(h_\theta(\mathbf{x}), y)}_{I_1} + \lambda \cdot \underbrace{\mathbb{E}_{(\mathbf{x}, y) \sim \mathcal{D}_n} L_M(r(\mathbf{x}; h_\theta); 0, \gamma_1)}_{I_2} \right. \\ \left. + \lambda \cdot \underbrace{\mathbb{E}_{(\mathbf{x}, y) \sim \mathcal{D}_s} L_M(r_{\text{c-s}}(\mathbf{x}; \Omega_y, h_\theta); -\gamma_2, \gamma_2)}_{I_3} \right\}, \quad (2)$$

where L_{CE} is the cross-entropy loss, $\lambda, \gamma_1, \gamma_2 > 0$ are hyperparameters, and $\mathcal{D} = \mathcal{D}_s \cup \mathcal{D}_n$, \mathcal{D}_s and \mathcal{D}_n denote the underlying distributions of all examples, cost-sensitive examples and normal examples, respectively. More specifically, Equation 2 consists of three terms: I_1 represents the cross-entropy loss with respect to h_θ over \mathcal{D} , which controls the overall accuracy, I_2 denotes the margin loss based on the standard certified radius, similar to the design of MACER, and I_3 optimizes the certified cost-sensitive robustness. The range of the interval $[l, r]$ used in the margin-based loss \mathcal{L}_M represents which data subpopulation we want to optimize. A larger thresholding parameter such as γ_2 lead to a higher data coverage, whereas the range with a smaller threshold includes fewer data points. We set $\gamma_2 > \gamma_1$ to have a wider adjustment range for sensitive seed examples. As shown in Wang et al. (2020), optimizing misclassified samples can help adversarial robustness. Thus, we intend to include the set of sensitive seed examples with a negative radius in $[-\gamma_2, 0)$ in the design of I_3 for better performance. Please refer to Appendix D.1 for further tuning details about how these two factors influence the final performance and how they interact with each other to affect controlled outcomes.

For pairwise cost matrices, we note that $[m] \setminus \Omega_y$ may contain classes other than the ground-truth class y . As a result, optimizing I_3 enhances prediction to non-cost-sensitive target classes $[m] \setminus \Omega_y$, which may lead to an undesirable degradation of overall accuracy. To solve this issue, we consider \mathcal{D} instead of \mathcal{D}_n in the objective of I_2 to particularly recalibrate the standard performance with the

Table 1: Certification results for seedwise cost matrices on CIFAR-10 and Imagenette. **Acc** stands for certified overall accuracy (%), and **Rob_{c-s}** refers to certified cost-sensitive robustness (%).

	CIFAR-10				Imagenette			
	<i>S-Seed</i> (3)		<i>M-Seed</i> (2, 4)		<i>S-Seed</i> (7)		<i>M-Seed</i> (3, 7)	
Method	Acc	Rob_{c-s}	Acc	Rob_{c-s}	Acc	Rob_{c-s}	Acc	Rob_{c-s}
Gaussian	65.4	22.3	65.9	29.3	80.3	64.6	80.4	58.9
SmoothMix	65.7	17.2	65.7	26.4	80.2	64.3	80.2	55.5
SmoothAdv	67.6	27.1	67.6	38.2	80.6	59.5	80.6	59.2
MACER	65.9	27.3	65.9	29.1	78.2	63.8	78.2	57.8
Gaussian-R	64.2	50.6	66.2	34.8	74.6	73.3	74.0	61.7
SmoothMix-R	63.2	48.9	63.7	28.1	77.6	66.6	76.1	68.9
SmoothAdv-R	66.1	53.5	66.5	47.1	76.1	68.9	77.6	60.5
Ours	66.1	62.8	66.4	46.8	79.6	81.1	79.2	71.5

non-sensitive groups. More concretely, we define the training objective for pairwise cost matrices by replacing the term I_2 in Equation 2 by:

$$I'_2 = \mathbb{E}_{(\mathbf{x}, y) \sim \mathcal{D}} \mathcal{L}_M(r(\mathbf{x}; h_\theta); 0, \gamma_1).$$

Note that by imposing different threshold restrictions $[l, u]$ on the certified radius of sensitive and non-sensitive seed classes, the learning process can prioritize making adjustments to data subpopulations of specific classes rather than considering all data points belonging to those classes. This is important for cost-sensitive learning with respect to the set of smoothed classifiers, and is one of the key advantages over the reweighting scheme typically used for standard cost-sensitive learning. As will be shown in our experiments, such a fine-grained optimization scheme enables our method to produce models with an improved certified cost-sensitive robustness without sacrificing overall accuracy.

5 Experiments

Settings. In our experiments, we evaluate our method on three image benchmarks: CIFAR-10 (Krizhevsky et al., 2009), Imagenette,¹ and the full ImageNet dataset (Deng et al., 2009). We also test our method on a medical dataset, HAM10k (Tschandl et al., 2018), to further examine its generalizability for real-world scenarios, where cost-sensitive misclassifications have more severe consequences. For CIFAR-10, ImageNet and HAM10k, we use the same ResNet architecture as used in Cohen et al. (2019). We choose ResNet-56 for CIFAR-10 and HAM10k, since it attains a comparable performance to ResNet-110 but with less computation costs, ResNet50 for ImageNet, and ResNet18 for Imagenette following Pethick et al. (2023). We focus on the setting of $\epsilon = 0.5$ and $\sigma = 0.5$ in our experiments since we observe similar trends in experiments under other settings (see Tables 6 and 7 in Appendix D.2 for results under $\epsilon = 0.25$ and $\sigma = 0.25$). For CIFAR10, Imagenette, and HAM10k, each setting is run on a single NVIDIA 40GB A100 GPU within one day. For the ImageNet dataset, each setting is conducted on four NVIDIA 40GB A100 GPUs over 1-2 days.

Methods. We compare our method with baseline randomized smoothing-based training methods, including the Gaussian Augmentation-based method (Cohen et al., 2019), denoted as Gaussian for short, SmoothAdv (Salman et al., 2019), SmoothMix (Jeong et al., 2021) and MACER (Zhai et al., 2020), and those adapted for cost-sensitive settings. Our method is developed based on MACER (Zhai et al., 2020), whereas we design Gaussian-R, SmoothAdv-R and SmoothMix-R by respectively adapting Gaussian, SmoothAdv and SmoothMix to cost-sensitive settings based on different reweighting schemes. In particular, Gaussian-R optimizes the base classifier, whereas both SmoothAdv-R and SmoothMix-R directly optimize the smoothed classifier. The aforementioned reweighting methods are optimized for cost-sensitive performance by tuning weight parameters associated with sensitive seed examples (see more details about these methods in Appendix B).

¹This dataset can be downloaded from <https://github.com/fastai/imagenette>.

Table 2: Certification results for pairwise cost matrices on CIFAR-10 and Imagenette. **Acc** stands for certified overall accuracy (%), and **Rob_{c-s}** refers to certified cost-sensitive robustness (%).

	CIFAR-10				Imagenette			
	<i>S-Pair</i> (3 → 5)		<i>M-Pair</i> (3 → 2, 4, 5)		<i>S-Pair</i> (7 → 2)		<i>M-Pair</i> (7 → 2, 4, 6)	
Method	Acc	Rob_{c-s}	Acc	Rob_{c-s}	Acc	Rob_{c-s}	Acc	Rob_{c-s}
Gaussian	65.4	50.4	65.4	33.6	80.3	88.5	80.3	75.6
SmoothMix	65.7	58.0	65.7	45.2	80.2	89.4	80.2	79.2
SmoothAdv	66.9	57.1	66.9	38.7	80.6	90.2	80.6	74.9
MACER	65.8	54.3	65.8	38.5	78.2	89.9	78.1	78.0
Gaussian-R	64.2	72.3	64.2	64.3	75.4	91.1	75.4	83.0
SmoothMix-R	63.2	67.5	63.2	46.2	77.6	89.7	77.3	82.6
SmoothAdv-R	66.1	80.4	64.9	75.3	78.6	90.7	77.6	80.4
Ours	67.3	92.4	65.2	82.2	79.6	93.8	79.6	86.3

Evaluation Metrics. We compare the performance of different methods based on two evaluation metrics, *certified cost-sensitive robustness* and *certified overall accuracy*. Certified cost-sensitive robustness $\text{Rob}_{c-s}(g_\theta) = \sum_{(x,y) \in \mathcal{S}^s} \mathbb{1}\{r_{c-s}(x; \Omega_y) > \epsilon\} / |\mathcal{S}^s|$ measures the ratio of cost-sensitive seed examples that are provably robust under ℓ_2 perturbations, where \mathcal{S}^s denotes the set of cost-sensitive seed examples. Certified overall accuracy $\text{Acc}(g_\theta) = \sum_{(x,y) \in \mathcal{S}} \mathbb{1}\{r(x) > 0\} / |\mathcal{S}|$ measures the fraction of correctly classified samples of the whole training dataset. In our experiments, we use $\max(\hat{r}_{\text{std}}, \hat{r}_{c-s})$ returned by Algorithm 1 as the empirical approximation of $r_{c-s}(x; \Omega_y)$ and use \hat{r}_{std} as the empirical estimate of $R(x)$. For all cost-sensitive learning methods, we choose the optimal tuning parameters based on the following selection criteria: it should yield a high Rob_{c-s} while Acc should be comparable to that of the baseline randomized smoothing methods designed for maximizing overall robustness (See Appendix D.1 for detailed results of hyperparameter tuning).

5.1 Main Results

Seedwise Cost Matrix. Table 1 reports the results on different seedwise cost matrices. In particular, we consider two types of seedwise cost matrices in our experiments: *S-Seed*: a randomly-selected sensitive seed class from all available classes, where we report the performance on the third class “cat” - label 3 for CIFAR-10 and “gas pump” - label 7 for Imagenette; and *M-Seed*: multiple sensitive seed classes, where “bird” - label 2 and “deer” - label 4 are considered as the sensitive seed classes for CIFAR-10, while we choose “chain saw” - label 3 and “gas pump” - label 7 for Imagenette. Table 1 demonstrates that our cost-sensitive robust training approach consistently surpasses all standard randomized smoothing baselines and their reweighting adaptations on cost-sensitive robustness. First of all, we observe that the reweighting adaptation is essential for standard randomized smoothing baselines to achieve much better cost-sensitive robustness. For instance, Gaussian-R improves Rob_{c-s} of the baseline method of Gaussian from 22.3% to 50.6% for the case of *S-Seed* (3). Nevertheless, our method still achieves the best cost-sensitive robustness of 62.8%, outperforming the strongest SmoothAdv-R adaptation method with an improvement of approximately 17.4%. Note that compared with other reweighting methods, our method achieves the best overall accuracy across all cost matrix settings. This suggests that our fine-grained thresholding techniques for optimizing certified radius achieve a more favorable trade-off between overall accuracy and cost-sensitive robustness compared to reweighting adaptations. In Appendix D, we show heatmap visualizations in Figure 5 to compare our method with MACER, which again confirms the effectiveness of our method.

Pairwise Cost Matrix. Similar to the seedwise case, we also consider two types of pairwise cost matrices: *S-Pair*: a randomly-selected sensitive seed class with one sensitive target class, and *M-Pair*: a single sensitive seed class with multiple sensitive target classes. Table 2 compares the performance of our method with randomized smoothing baselines for different pairwise cost matrices. Here, the cost-sensitive pairwise transformations are depicted in the bracket. For example, *S-Pair* (3 → 5) stands for the scenario where only misclassifications from “cat” - label 3 to “dog” - label 5 will incur a cost. It can be seen from Table 2 that our method consistently achieves the best certified cost-sensitive

Table 3: Certification results (%) for various seedwise cost matrices on ImageNet and HAM10k.

	ImageNet						HAM10k	
	<i>M-Seed</i> (44, 48)		<i>S-Seed</i> (919)		<i>S-Seed</i> (920)		<i>S-Seed</i> (0)	
Method	Acc	Rob_{c-s}	Acc	Rob_{c-s}	Acc	Rob_{c-s}	Acc	Rob_{c-s}
Gaussian	58.4	45.0	58.4	58.0	58.4	52.0	82.9	11.8
SmoothAdv	57.1	38.0	57.1	70.0	57.1	67.0	82.4	10.0
MACER	58.5	40.0	58.5	66.0	58.5	62.0	82.8	25.0
Gaussian-R	48.6	53.0	52.4	78.0	51.0	62.0	80.5	19.7
SmoothAdv-R	50.4	41.0	50.6	76.0	52.4	78.0	78.3	40.1
Ours	54.2	61.0	53.4	84.0	53.6	76.0	83.1	42.7

robustness without sacrificing overall accuracy. Similar to the seedwise scenarios, the standard randomized smoothing baselines, primarily designed for overall robustness, fall short in certifying cost-sensitive robustness. The reweighting adaptations of baseline randomized smoothing methods exhibit improved performance in cost-sensitive robustness but at the expense of a notable decline in overall accuracy. For instance, in the *S-Pair* (3 \rightarrow 5) scenario, our method achieves a 92.4% certified cost-sensitive robustness, significantly outperforming SmoothAdv-R with a robustness performance of 80.4%. This improvement over reweighting baselines in pairwise scenarios can be attributed to the design of our method that optimizes the cost-sensitive certified radius $r_{c-s}(\mathbf{x}; \Omega_y)$.

ImageNet. We evaluate the scalability and performance of our method on the full ImageNet dataset. The results are shown in Table 3, where $\epsilon = 0.5$ and $\sigma = 0.5$. We consider three meaning seedwise cost matrix scenarios: *S-Seed* (919) being street sign, *S-Seed* (920) denoting traffic light and signals, and *M-Seeds* (44, 48) representing different types of giant lizards. Misclassifications of images from these ImageNet classes could cause significant consequences in autonomous driving or danger in the real world. We can observe from Table 3 that our method obtains a better trade-off between overall accuracy and cost-sensitive robustness across various cost-matrix settings.

HAM10k. We examine the performance of our method on HAM10k (Tschandl et al., 2018), an imbalanced skin cancer dataset with 7 classes. Due to the small sample size, we group all images from the benign classes into a larger single category and all images from the malignant classes into another, which formulates a binary classification task. Since misclassifying a malignant tumor as benign typically has more severe consequences and results in higher costs for this medical application, we set any misclassification from malignant to benign as cost-sensitive, while regarding the cost of the other type of misclassifications as 0. The results are depicted in the last column of Table 3. Similar to previous experiments, we set $\epsilon = 0.5$ and $\sigma = 0.5$. Notably, SmoothAdv-R and our method are the top-2 methods for promoting cost-sensitive robustness. However, SmoothAdv-R depicts a 4% decline in accuracy compared to the Gaussian baseline, whereas our approach achieves a more desirable trade-off between the two metrics, underscoring its effectiveness for real-world applications.

5.2 Further Analysis

Results with Varying ϵ . To visualize the consistency of our improvement, we compare the certified accuracy curves of sensitive seed examples with varying size of l_2 perturbations for the aforementioned methods in Figure 1. The performance at $\epsilon = 0$ measures the certified accuracy for cost-sensitive examples drawn from \mathcal{D}_s . It is evident that our method consistently outperforms all the baseline methods and their adaptations in certified cost-sensitive accuracy across different ϵ . Note that the certified accuracy at $\epsilon = 0.5$ aligns with Rob_{c-s} as presented in Tables 1 and 2. In particular, we observe a significant improvement at $\epsilon = 0.5$ of our method compared with other baselines, further corroborating our conclusions discussed in Section 5.1.

Trade-off Comparisons. To further illustrate the advantages of our method in achieving a more desirable accuracy-robustness trade-off, we compare the performance of our method with others and visualize it in Figures 2(a) and 2(b). Each dot is a model produced by a certified robust training method, where its performance is depicted as a (Acc, Rob_{c-s}) pair. In particular, we compare Gaussian-R

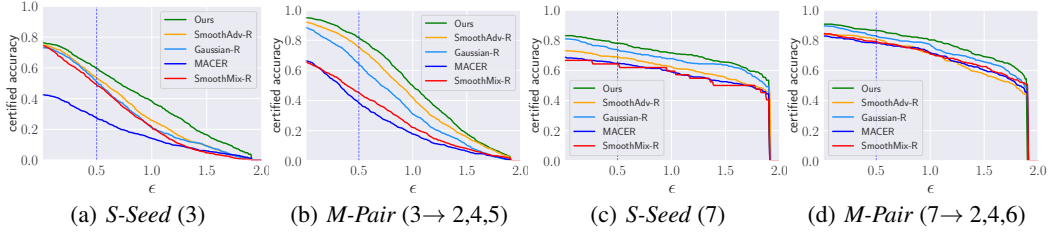


Figure 1: Certified accuracy curves for varying ϵ on different datasets under different cost matrix settings. Figures (a) and (b) are results for CIFAR-10, while Figures (c) and (d) are for Imagenette.

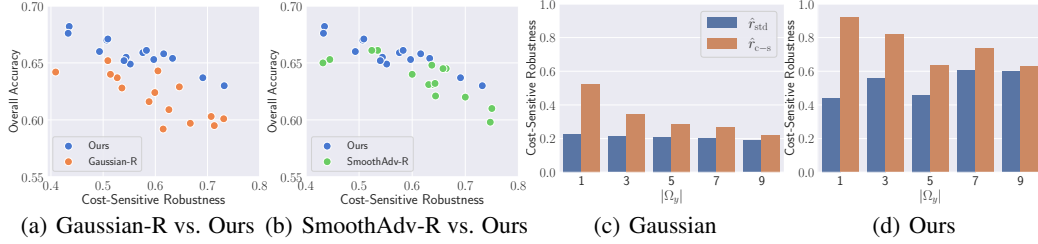


Figure 2: Figures (a) and (b) showcase the trade-off between overall accuracy and cost-sensitive robustness. Figures (c) and (d) compare the cost-sensitive robustness computed using \hat{r}_{std} and $\hat{r}_{\text{c-s}}$.

and SmoothAdv-R with our method under the cost-sensitive setting of *S-Seed* (3), where we vary the tuning hyperparameters for each method to obtain multiple models. As shown in the figure, the distribution of the models produced by our method appears in the top right part of the figure, indicating a more favorable trade-off compared with the two baselines, which inevitably sacrifice the overall accuracy performance to a large degree to achieve a desirable cost-sensitive robustness.

Comparing $\hat{r}_{\text{c-s}}$ with \hat{r}_{std} . Recall in Section 3.2, we put forward a practical certification algorithm which is designed to produce a tight cost-sensitive robustness guarantee by returning $\max(\hat{r}_{\text{std}}, \hat{r}_{\text{c-s}})$. To further illustrate the advantages of $\hat{r}_{\text{c-s}}$ over \hat{r}_{std} , we conduct experiments to compare the certified cost-sensitive robustness computed based on \hat{r}_{std} and $\hat{r}_{\text{c-s}}$ across different cost matrix scenarios. The results are shown in Figures 2(c) and 2(d). We fix a single seed class “cat” as sensitive and vary the size of its corresponding cost-sensitive target classes, randomly selecting $|\Omega_y| \in \{1, 3, 5, 7, 9\}$ of all the possible target classes. We then evaluate the performance of the models produced by Gaussian as well as our method. Our results show that the cost-sensitive robustness defined by $\hat{r}_{\text{c-s}}$ outperforms that of \hat{r}_{std} across all of the settings, and the performance gap is more pronounced as the size of Ω_y decreases. This phenomenon is because when $|\Omega_y|$ is small, the runner-up class is very likely not to be covered by Ω_y , which further suggests that $\overline{p_B}$, the estimated probability of the top class in Ω_y , could be much lower than the probability of the runner-up class $\max_{k \neq y} [h_\theta(\mathbf{x})]_k$ as used for computing \hat{r}_{std} . These results underscore the superiority of $\hat{r}_{\text{c-s}}$ and the importance of our algorithm for certifying cost-sensitive robustness. However, when $|\Omega_y|$ contains the runner-up class in $[m]$, as discussed in Remark 3.5, $\hat{r}_{\text{c-s}}$ can be smaller than \hat{r}_{std} . We provide further empirical evidence about the percentage for $\hat{r}_{\text{std}} > \hat{r}_{\text{c-s}}$ across different cost matrix setting in Table 8 in Appendix D.3.

6 Conclusion

We developed a general method to certify and train for cost-sensitive robustness under the randomized smoothing framework. Built upon the notion of cost-sensitive certified radius and fine-grained thresholding techniques for optimizing the certified radius with different data subgroups, our method significantly improves the certified robustness for cost-sensitive transformations. Experiments on image benchmarks and a real-world medical dataset demonstrate the superiority of our approach compared to various baselines. Compared with other reweighting-based approaches, our method achieves a more desirable trade-off between overall accuracy and certified cost-sensitive robustness. Our work opens up new possibilities for building better robust models for cost-sensitive applications.

References

- Kaiser Asif, Wei Xing, Sima Behpour, and Brian D Ziebart. Adversarial cost-sensitive classification. In *UAI*, pp. 92–101, 2015.
- Anish Athalye, Nicholas Carlini, and David Wagner. Obfuscated gradients give a false sense of security: Circumventing defenses to adversarial examples. In *International conference on machine learning*, pp. 274–283. PMLR, 2018.
- Nicholas Carlini and David Wagner. Towards evaluating the robustness of neural networks. In *2017 IEEE Symposium on Security and Privacy (SP)*, pp. 39–57. Ieee, 2017.
- Nicholas Carlini, Florian Tramer, Krishnamurthy Dj Dvijotham, Leslie Rice, Mingjie Sun, and J Zico Kolter. (certified!!) adversarial robustness for free! In *The Eleventh International Conference on Learning Representations*, 2022.
- Yair Carmon, Aditi Raghunathan, Ludwig Schmidt, John C Duchi, and Percy S Liang. Unlabeled data improves adversarial robustness. *Advances in neural information processing systems*, 32, 2019.
- Yizheng Chen, Shiqi Wang, Weifan Jiang, Asaf Cidon, and Suman Jana. Cost-aware robust tree ensembles for security applications. In *USENIX Security Symposium*, pp. 2291–2308, 2021.
- Jeremy Cohen, Elan Rosenfeld, and Zico Kolter. Certified adversarial robustness via randomized smoothing. In *international conference on machine learning*, pp. 1310–1320. PMLR, 2019.
- Jia Deng, Wei Dong, Richard Socher, Li-Jia Li, Kai Li, and Li Fei-Fei. Imagenet: A large-scale hierarchical image database. In *2009 IEEE conference on computer vision and pattern recognition*, pp. 248–255. Ieee, 2009.
- Pedro Domingos. Metacost: A general method for making classifiers cost-sensitive. In *Proceedings of the fifth ACM SIGKDD international conference on Knowledge discovery and data mining*, pp. 155–164, 1999.
- Charles Elkan. The foundations of cost-sensitive learning. In *International joint conference on artificial intelligence*, volume 17, pp. 973–978. Lawrence Erlbaum Associates Ltd, 2001.
- Ian J Goodfellow, Jonathon Shlens, and Christian Szegedy. Explaining and harnessing adversarial examples. *arXiv preprint arXiv:1412.6572*, 2014.
- Sven Gowal, Krishnamurthy Dvijotham, Robert Stanforth, Rudy Bunel, Chongli Qin, Jonathan Uesato, Relja Arandjelovic, Timothy Mann, and Pushmeet Kohli. On the effectiveness of interval bound propagation for training verifiably robust models. *arXiv preprint arXiv:1810.12715*, 2018.
- Jongheon Jeong, Sejun Park, Minkyu Kim, Heung-Chang Lee, Do-Guk Kim, and Jinwoo Shin. Smoothmix: Training confidence-calibrated smoothed classifiers for certified robustness. *Advances in Neural Information Processing Systems*, 34:30153–30168, 2021.
- Jinyuan Jia, Xiaoyu Cao, Binghui Wang, and Neil Zhenqiang Gong. Certified robustness for top-k predictions against adversarial perturbations via randomized smoothing. *arXiv preprint arXiv:1912.09899*, 2019.
- Salman H Khan, Munawar Hayat, Mohammed Bennamoun, Ferdous A Sohel, and Roberto Togneri. Cost-sensitive learning of deep feature representations from imbalanced data. *IEEE transactions on neural networks and learning systems*, 29(8):3573–3587, 2017.
- Alex Krizhevsky, Geoffrey Hinton, et al. Learning multiple layers of features from tiny images. 2009.
- Alexey Kurakin, Ian Goodfellow, and Samy Bengio. Adversarial machine learning at scale. *arXiv preprint arXiv:1611.01236*, 2016.
- Mathias Lecuyer, Vaggelis Atlidakis, Roxana Geambasu, Daniel Hsu, and Suman Jana. Certified robustness to adversarial examples with differential privacy. In *2019 IEEE Symposium on Security and Privacy (SP)*, pp. 656–672. IEEE, 2019.

- Bai Li, Changyou Chen, Wenlin Wang, and Lawrence Carin. Certified adversarial robustness with additive noise. *Advances in neural information processing systems*, 32, 2019.
- Xuanqing Liu, Minhao Cheng, Huan Zhang, and Cho-Jui Hsieh. Towards robust neural networks via random self-ensemble. In *Proceedings of the European Conference on Computer Vision (ECCV)*, pp. 369–385, 2018.
- Aleksander Madry, Aleksandar Makelov, Ludwig Schmidt, Dimitris Tsipras, and Adrian Vladu. Towards deep learning models resistant to adversarial attacks. *arXiv preprint arXiv:1706.06083*, 2017.
- Nicolas Papernot, Patrick McDaniel, Xi Wu, Somesh Jha, and Ananthram Swami. Distillation as a defense to adversarial perturbations against deep neural networks. In *2016 IEEE symposium on security and privacy (SP)*, pp. 582–597. IEEE, 2016.
- Thomas Pethick, Grigorios Chrysos, and Volkan Cevher. Revisiting adversarial training for the worst-performing class. *Transactions on Machine Learning Research*, 2023. ISSN 2835-8856.
- Aaditya Raghunathan, Jacob Steinhardt, and Percy Liang. Certified defenses against adversarial examples. In *International Conference on Learning Representations*, 2018.
- Hadi Salman, Jerry Li, Ilya Razenshteyn, Pengchuan Zhang, Huan Zhang, Sebastien Bubeck, and Greg Yang. Provably robust deep learning via adversarially trained smoothed classifiers. *Advances in Neural Information Processing Systems*, 32, 2019.
- Christian Szegedy, Wojciech Zaremba, Ilya Sutskever, Joan Bruna, Dumitru Erhan, Ian Goodfellow, and Rob Fergus. Intriguing properties of neural networks. *arXiv preprint arXiv:1312.6199*, 2013.
- Philipp Tschandl, Cliff Rosendahl, and Harald Kittler. The ham10000 dataset, a large collection of multi-source dermatoscopic images of common pigmented skin lesions. *Scientific data*, 5(1):1–9, 2018.
- Yisen Wang, Difan Zou, Jinfeng Yi, James Bailey, Xingjun Ma, and Quanquan Gu. Improving adversarial robustness requires revisiting misclassified examples. In *International Conference on Learning Representations*, 2020.
- Eric Wong and Zico Kolter. Provable defenses against adversarial examples via the convex outer adversarial polytope. In *International conference on machine learning*, pp. 5286–5295. PMLR, 2018.
- Eric Wong, Frank Schmidt, Jan Hendrik Metzen, and J Zico Kolter. Scaling provable adversarial defenses. *Advances in Neural Information Processing Systems*, 31, 2018.
- Chaowei Xiao, Zhongzhu Chen, Kun Jin, Jiongxiao Wang, Weili Nie, Mingyan Liu, Anima Anandkumar, Bo Li, and Dawn Song. Densepure: Understanding diffusion models for adversarial robustness. In *The Eleventh International Conference on Learning Representations*, 2022.
- Runtian Zhai, Chen Dan, Di He, Huan Zhang, Boqing Gong, Pradeep Ravikumar, Cho-Jui Hsieh, and Liwei Wang. Macer: Attack-free and scalable robust training via maximizing certified radius. In *International Conference on Learning Representations*, 2020.
- Hongyang Zhang, Yaodong Yu, Jiantao Jiao, Eric Xing, Laurent El Ghaoui, and Michael Jordan. Theoretically principled trade-off between robustness and accuracy. In *International conference on machine learning*, pp. 7472–7482. PMLR, 2019.
- Jiawei Zhang, Zhongzhu Chen, Huan Zhang, Chaowei Xiao, and Bo Li. {DiffSmooth}: Certifiably robust learning via diffusion models and local smoothing. In *32nd USENIX Security Symposium (USENIX Security 23)*, pp. 4787–4804, 2023.
- Xiao Zhang and David Evans. Cost-sensitive robustness against adversarial examples. In *International Conference on Learning Representations*, 2019.

Appendix

A Proofs of Main Results in Section 3

A.1 Proof of Theorem 3.2

Proof of Theorem 3.2. Recall that standard certified radius is defined as:

$$r(\mathbf{x}) = \frac{\sigma}{2} \left[\Phi^{-1}([h_\theta(\mathbf{x})]_y) - \Phi^{-1}\left(\max_{k \neq y} [h_\theta(\mathbf{x})]_k\right) \right], \quad (3)$$

Note that \mathbf{x} is assumed to be correctly classified by g_θ in the definition of $r(\mathbf{x})$, suggesting that the ground-truth y is also the top-1 class. In addition, our *cost-sensitive certified radius* is defined as:

$$r_{c-s}(\mathbf{x}; \Omega_y) = \frac{\sigma}{2} \left[\Phi^{-1}\left(\max_{k \in [m]} [h_\theta(\mathbf{x})]_k\right) - \Phi^{-1}\left(\max_{k \in \Omega_y} [h_\theta(\mathbf{x})]_k\right) \right],$$

Depending on the cardinality of Ω_y , we have the following observations:

- When $|\Omega_y| = m - 1$, $r_{c-s}(\mathbf{x}; \Omega_y) \Leftrightarrow r(\mathbf{x})$. Since $\Omega_y = \{j | j \neq y, j \in [m]\}$ encompasses all incorrect classes, the two probability terms are fully matched for both radius.
- When $|\Omega_y| < m - 1$, $r_{c-s}(\mathbf{x}; \Omega_y) \geq r(\mathbf{x})$. This is because the class index scope in the second term of $r_{c-s}(\mathbf{x}; \Omega_y)$ is narrower than that in $r(\mathbf{x})$. Since $\Omega_y \subseteq \{j \neq y, j \in [m]\}$, the highest probability with respect to $|\Omega_y|$ will be not greater than the highest probability related to all incorrect classes in $r(\mathbf{x})$. Consequently, $r_{c-s}(\mathbf{x}; \Omega_y) \geq r(\mathbf{x})$.

Therefore, we complete the proof of Theorem 3.2. □

A.2 Proof of Theorem 3.3

Proof of Theorem 3.3. Our goal is to show that \hat{r}_{c-s} specified in Algorithm 1 is a cost-sensitive certified radius with at least $1 - \alpha$ confidence over the randomness of the Gaussian sampling. Let m be the total number of label classes, and let (p_1, \dots, p_m) be the ground-truth probability distribution of the smoothed classifier g_θ for a given example (\mathbf{x}, y) . Denote by p_A, p_B the maximum probabilities in $[m]$ and in Ω_y , respectively. According to the design of Algorithm 1, we can compute the empirical estimate of p_k for any $k \in [m]$ based on n Gaussian samples and the base classifier f_θ . Let $(\hat{p}_1, \dots, \hat{p}_m)$ be the corresponding empirical estimates, then we immediately know

$$\hat{p}_k \sim \text{Binomial}(n, p_k), \text{ for any } k \in [m].$$

For \hat{r}_{std} , we follow the same procedure as in Cohen et al. (2019) to compute the $1 - \alpha$ lower confidence bound on p_A , which is guaranteed by the fact that $p_B \leq 1 - p_A$. However, for the computation of \hat{r}_{c-s} , we need compute both a lower confidence bound on p_A and an upper confidence bound on p_B , which requires additional care to make the computation rigorous. In particular, we adapt the definition of standard certified radius (Theorem 1 in Cohen et al. (2019)) to cost-sensitive scenarios for deriving \hat{r}_{c-s} . Based on the construction $\underline{p}_A = \text{LOWERCONFBOUND}(\text{count}[\hat{c}_A], n, 1 - \alpha/2)$, we have

$$\Pr \left[\underline{p}_A \leq p_A \right] \geq 1 - \frac{\alpha}{2}.$$

Therefore, the remaining task is to prove

$$\Pr \left[\overline{p}_B \geq p_B \right] \geq 1 - \frac{\alpha}{2}, \quad (4)$$

where \overline{p}_B is defined according to line 14 of Algorithm 1, and Ω_y denotes the set of cost-sensitive target classes. Note that $p_B = \max_{k \in \Omega_y} \{p_k\}$ is used to define $r_{c-s}(\mathbf{x}, \Omega_y)$. If the above inequality holds true, we immediately know that by union bound,

$$\begin{aligned} \Pr \left[\hat{r}_{c-s} \leq r_{c-s}(\mathbf{x}; \Omega_y) \right] &= \Pr \left[\frac{\sigma}{2} (\Phi^{-1}(\underline{p}_A) - \Phi^{-1}(\overline{p}_B)) \leq \frac{\sigma}{2} (\Phi^{-1}(p_A) - \Phi^{-1}(p_B)) \right] \\ &\geq 1 - \left(\Pr \left[\underline{p}_A \geq p_A \right] + \Pr \left[\overline{p}_B \leq p_B \right] \right) \geq 1 - \alpha. \end{aligned}$$

The challenge for proving Equation 4 lies in the that we do not know the top class within Ω_y which is different from the case of p_A . Therefore, we resort to upper bound the maximum over all the ground-truth class probabilities within Ω_y . Based on the distribution of \hat{p}_k , we know for any $k \in \Omega_y$,

$$\Pr\left[\overline{p}_k \geq p_k\right] \geq 1 - \alpha/(2|\Omega_y|),$$

where \overline{p}_k is defined as the $1 - \alpha/(2|\Omega_y|)$ upper confidence bound computed using \hat{p}_k . We remark that the choice of $1 - \alpha/(2|\Omega_y|)$ can in fact be varied for each $k \in \Omega_y$ and even optimized for obtaining tighter bounds, as long as the summation of the probabilities of bad event happening is at most $\alpha/2$. Here, we choose the same value of $1 - \alpha/(2|\Omega_y|)$ across different k only for simplicity. According to union bound, we have

$$\begin{aligned} \Pr\left[\max_{k \in \Omega_y} \overline{p}_k \geq p_B\right] &= \Pr\left[\max_{k \in \Omega_y} \overline{p}_k \geq \max_{k \in \Omega_y} p_k\right] \geq 1 - \sum_{k \in \Omega_y} \Pr\left[\overline{p}_k \leq p_k\right] \\ &\geq 1 - |\Omega_y| \cdot \alpha/(2|\Omega_y|) = 1 - \frac{\alpha}{2}, \end{aligned}$$

where the first inequality holds because of union bound, which completes the proof. \square

B Reweighting Adaptation of Randomized-Smoothing Baselines

We explain the reweighting technique we used to adapt different standard randomized smoothing baselines. Given a binary cost matrix, \mathcal{D} is the underlying data distribution, let \mathcal{D}_s be the distribution of all sensitive examples which incur costs if misclassified and let \mathcal{D}_n represent the distribution of the remaining normal examples.

Gaussian-R. We consider the base classifier training method introduced in Cohen et al. (2019), which proposes to inject Gaussian noise to all inputs during the training process of f_θ . Intuitively, the reweighting scheme to adapt Gaussian method to cost-sensitive settings is to increase the weights assigned to the loss function of sensitive examples, denoted as Gaussian-R. More concretely, the training objective of Gaussian-R is defined as follows:

$$\min_{\theta \in \Theta} \left[\mathbb{E}_{(\mathbf{x}, y) \sim \mathcal{D}_n} \mathbb{E}_\delta \mathcal{L}_{\text{CE}}(f_\theta(\mathbf{x} + \delta), y) + \alpha \cdot \mathbb{E}_{(\mathbf{x}, y) \sim \mathcal{D}_s} \mathbb{E}_\delta \mathcal{L}_{\text{CE}}(f_\theta(\mathbf{x} + \delta), y) \right].$$

where Θ denotes the set of model parameters, \mathcal{L}_{CE} represents the cross-entropy loss, and $\alpha \geq 1$ is a trade-off parameter that controls the performance between sensitive and non-sensitive examples. When $\alpha = 1$, the above objective function is equivalent to the training loss used in standard randomized smoothing.

SmoothAdv-R. SmoothAdv (Salman et al., 2019) applies adversarial training to Gaussian smoothed classifiers h_θ to improve the overall certified robustness. The adaptation of the reweighting technique on SmoothAdv is similar to that of Gaussian-R:

$$\min_{\theta \in \Theta} \left[\mathbb{E}_{(\mathbf{x}, y) \sim \mathcal{D}_n} \mathbb{E}_\delta \mathcal{L}_{\text{CE}}(h_\theta(\mathbf{x}' + \delta), y) + \alpha \cdot \mathbb{E}_{(\mathbf{x}, y) \sim \mathcal{D}_s} \mathbb{E}_\delta \mathcal{L}_{\text{CE}}(h_\theta(\mathbf{x}' + \delta), y) \right],$$

where α is a trade-off parameter, h_θ represents the smoothed soft classifier which has the same meaning in Definition 3.1, \mathbf{x}' represents an adversarial example against smoothed classifiers h_θ , and the adversarial attack process can be formulated as:

$$\mathbf{x}' = \arg \max_{\|\tilde{\mathbf{x}} - \mathbf{x}\|_2 \leq \epsilon} \mathcal{L}_{\text{CE}}(h_\theta(\tilde{\mathbf{x}} + \delta), y) = \arg \max_{\|\tilde{\mathbf{x}} - \mathbf{x}\|_2 \leq \epsilon} \left(-\log \mathbb{E}_{\delta \sim \mathcal{N}(0, \sigma^2 \mathbf{I})} [f_\theta(\tilde{\mathbf{x}} + \delta)]_y \right). \quad (5)$$

Due to the intractability of Gaussian distributions, the computation of h_θ can be achieved by one-order approximations:

$$\mathbb{E}_{\delta \sim \mathcal{N}(0, \sigma^2 \mathbf{I})} [f_\theta(\mathbf{x}' + \delta)]_y \approx \frac{1}{m} \sum_{i=1}^m [f_\theta(\mathbf{x}' + \delta_i)]_y, \quad (6)$$

where m represents the number of Gaussian noises for one input to approximate the smoothed classifier, ϵ represents the ℓ_2 distance between the adversarial example \mathbf{x}' and \mathbf{x} . Here, $\delta_1, \delta_2 \dots \delta_m \sim \mathcal{N}(0, \sigma^2 \mathbf{I})$ are sampled *i.i.d* from the spherical Gaussian distribution.

SmoothMix-R. SmoothMix (Jeong et al., 2021) finds that the *over-confident but semantically off-class* samples harm the classifier’s training, so it labels it as the uniform confidence. The training objective goes like this:

$$\mathcal{L}^{\text{nat}} + \eta \cdot \mathcal{L}^{\text{mix}} = \min_{\theta \in \Theta} \left[\mathbb{E}_{(\mathbf{x}, y) \sim \mathcal{D}} \mathbb{E}_{\delta} \mathcal{L}_{\text{CE}}(f_{\theta}(\mathbf{x} + \delta), y) + \eta \cdot \mathbb{E}_{(\mathbf{x}, y) \sim \mathcal{D}} \mathbb{E}_{\delta} \mathcal{L}_{\text{CE}}(h_{\theta}(\mathbf{x}^{\text{mix}} + \delta), y^{\text{mix}}) \right].$$

The left part of the equation \mathcal{L}^{nat} represents the natural loss which controls overall accuracy, and the right part \mathcal{L}^{mix} represents the confidence-calibrated loss which controls overall robustness. For our reweighting adaptation, we modify the second loss to rebalance the robustness of cost-sensitive examples and normal examples:

$$\min_{\theta \in \Theta} \left[\mathbb{E}_{(\mathbf{x}, y) \sim \mathcal{D}_n} \mathbb{E}_{\delta} \mathcal{L}_{\text{CE}}(f_{\theta}(\mathbf{x}^{\text{mix}} + \delta), y^{\text{mix}}) + \alpha \cdot \mathbb{E}_{(\mathbf{x}, y) \sim \mathcal{D}_s} \mathbb{E}_{\delta} \mathcal{L}_{\text{CE}}(h_{\theta}(\mathbf{x}^{\text{mix}} + \delta), y^{\text{mix}}) \right].$$

We refer Jeong et al. (2021) to readers for detailed discussions on the computation of the confidence calibration process and the construction of $(\mathbf{x}^{\text{mix}}, y^{\text{mix}})$.

C Comparisons with Alternative Method

We compare our method with Zhang & Evans (2019)’s, which provides a way to certify and train for cost-sensitive robustness based on the convex relaxation-based method (Wong & Kolter, 2018). However, the initial work of Wong & Kolter (2018) only focuses on ℓ_{∞} -norm bounded perturbations and does not consider perturbations in ℓ_2 -norm. Therefore, the proposed method in Zhang & Evans (2019) is not applicable to certify cost-sensitive robustness for ℓ_2 perturbations. We note that in a follow-up work of Wong et al. (2018), they extend the developed certification techniques to ℓ_2 perturbations. For a fair comparison with our method, we adapt the cost-sensitive robust learning method of Zhang & Evans (2019) to handle ℓ_2 -norm perturbations using the method of Wong et al. (2018). We report their comparisons in Table 4, the certified cost-sensitive robustness for the convex-relaxation method is computed as the *cost-sensitive robust error* defined in Zhang & Evans (2019). Table 4 shows that our method achieves much higher overall accuracy even against larger ℓ_2 perturbations, suggesting better cost-sensitive robustness and overall accuracy trade-off. Also, we find in our implementation that convex relaxation-based methods is not applicable to large ℓ_2 perturbations (e.g., $\epsilon = 0.5$), due to memory issues.

Table 4: Comparisons (%) of our method with convex relaxation based method (Zhang & Evans, 2019) on CIFAR-10, where a single pairwise transformation *S-Pair* ($3 \rightarrow 5$) is considered sensitive.

Method	ℓ_2 noise	Acc	Rob _{c-s}
Zhang & Evans (2019)	$\epsilon = 0.25$	48.0	94.4
Ours	$\epsilon = 0.5$	67.3	92.4

D Additional Experimental Details and Results

Other Details of Algorithm 1. We follow the same sampling procedure of Cohen et al. (2019). To be more specific, the sampling function $\text{SAMPLEUNDERNOISE}(f, \mathbf{x}, n, \sigma)$ is defined as:

1. Draw n i.i.d. samples of Gaussian noises $\delta_1 \dots \delta_n \sim \mathcal{N}(0, \sigma^2 \mathbf{I})$.
2. Obtain the predictions $f(\mathbf{x} + \delta_1), \dots, f(\mathbf{x} + \delta_n)$ with base classifier f on noisy images.
3. Return the counts for each class, where the count for class c is $\sum_{i \in [n]} \mathbb{1}[f(\mathbf{x} + \delta_i) = c]$.

D.1 Hyperparameter Tuning

The choice of hyperparameters plays a critical role in cost-sensitive learning. For Gaussian-R, SmoothAdv-R and SmoothMix-R, the weight parameter α is carefully tuned to ensure the best trade-off between overall accuracy and cost-sensitive robustness, where we enumerate all values from

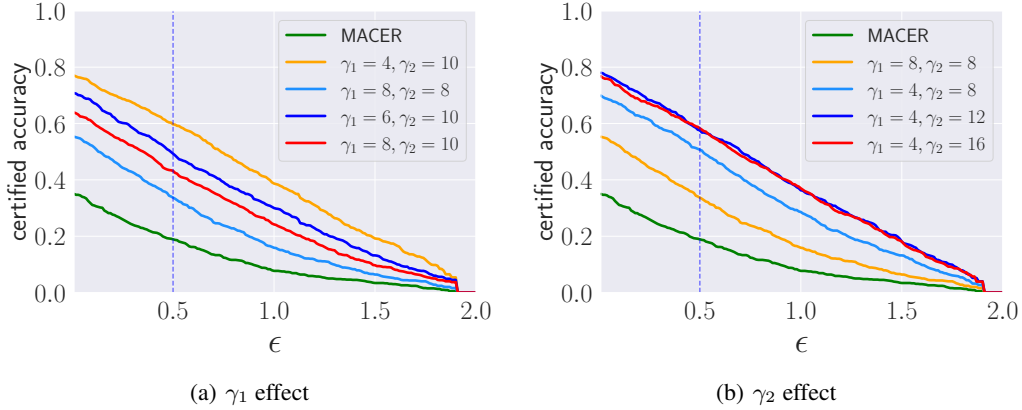


Figure 3: Visualizations of our method with MACER in cost-sensitive performance. Figure 3(a) fix $\gamma_2 = 10$ and vary $\gamma_1 \in \{4, 6, 8\}$. Figure 3(b) fix $\gamma_1 = 4$ and vary $\gamma_2 \in \{8, 12, 16\}$. The cost matrix is set as the matrix representing a single cost-sensitive seed class “Cat”.

$\{1.0, 1.1, \dots, 2.0\}$ and observe that nearly in all cases of cost matrices, setting $\alpha = 1.1$ achieves the best result. For our method, we follow Zhai et al. (2020)’s setup for training. The main difference between our method and MACER is the choice of γ . MACER uses $\gamma = 8$ to enhance the overall robustness for all classes, whereas we set $\gamma_1 = 4$ for normal classes and $\gamma_2 = 16$ for sensitive classes based on our analysis in Section 4.

In this section, we study the effect of hyperparameters γ_1 and γ_2 used in our method proposed in Section 4 on the two evaluation metrics, certified overall accuracy and cost-sensitive robustness. Note that our goal is to improve cost-sensitive robustness without sacrificing overall accuracy, where γ_1 controls the margin of normal classes and γ_2 controls the margin of sensitive classes. In particular, we report the parameter tuning results on CIFAR-10. Here, the cost matrix is selected as a seedwise cost matrix with a sensitive seed class “cat”. We choose the specific “cat” class only for illustration purposes, as we observe similar trends in our experiments for other cost matrices, similar to the results shown in Table 1. In addition, we consider two comparison baselines:

1. MACER (Zhai et al., 2020) with $\gamma = 8$, restricting only on correctly classified examples, with $(\mathbf{Acc}, \mathbf{Rob}_{e-s})$ being (64.7%, 18.9%).
2. Our method with $\gamma_1 = 8$ and $\gamma_2 = 8$, with $(\mathbf{Acc}, \mathbf{Rob}_{e-s})$ being (66.0%, 33.8%). The only difference with MACER is the inclusion of misclassified samples for sensitive seed classes.

Below, we show the effect of γ_1 and γ_2 on the performance of our method, respectively.

Effect of γ_1 . Note that γ_1 is used to restrict the certified radius with respect to normal data points. Figure 3(a) illustrates the influence of varying $\gamma_1 \in \{4, 6, 8\}$ and fixed $\gamma_2 = 10$ for our method, with comparisons to the two baselines.

For the original implementation of MACER, γ is selected as 8 for the best overall performance. Although it achieves good overall robustness, it does not work for cost-sensitive settings, which suggests the possibility of a trade-off space, where different classes can be balanced to achieve our desired goal of cost-sensitive robustness. The second baseline is our method with $\gamma_1 = 8$ and $\gamma_2 = 8$. By incorporating misclassified samples for sensitive seed class, the cost-sensitive performance substantially improves. These results show the significance of including misclassified sensitive samples during the optimization process of the certified radius. Moreover, we can observe from Figure 3(a) that as we reduce the value of γ_1 , the robustness performance of the cost-sensitive seed class increases. This again confirms that by limiting the certified radius of normal classes to a small threshold in our method, the model can prioritize sensitive classes and enhance cost-sensitive robustness. As depicted in Table 5, the overall certified accuracy shows negligible variation, underscoring the efficacy of our training method in preserving overall accuracy.

Table 5: Performance (%) of our method for different combinations of γ_1 and γ_2 . Here, the cost-sensitive scenario is captured by the seedwise cost matrix with a single sensitive seed class ‘‘Cat’’ for CIFAR-10.

	$\gamma_2 = 8$		$\gamma_2 = 10$		$\gamma_2 = 12$		$\gamma_2 = 16$	
	Acc	Rob _{c-s}	Acc	Rob _{c-s}	Acc	Rob _{c-s}	Acc	Rob _{c-s}
$\gamma_1 = 2$	65.4	63.3	63.4	68.7	63.7	69.1	63.0	70.5
$\gamma_1 = 4$	67.0	50.7	65.3	59.7	65.9	57.6	66.1	58.3
$\gamma_1 = 6$	67.3	39.6	66.0	49.3	65.5	54.4	64.9	55.2
$\gamma_1 = 8$	66.0	33.8	65.0	43.2	64.1	47.4	64.5	46.3

Effect of γ_2 . Figure 3(b) illustrates the influence of varying $\gamma_2 \in \{8, 12, 16\}$ with fixed $\gamma_1 = 4$ for our method, with comparisons to the two baselines, on both overall accuracy and cost-sensitive robustness. Moreover, we can observe that as we increase the value of γ_2 , the robustness performance of the cost-sensitive seed class increases. This confirms that by optimizing the certified radius of sensitive classes to a large threshold in our method, the model can focus more on sensitive classes and enhance cost-sensitive robustness. Additionally, there is a slight increase in the overall certified accuracy. This can be attributed to the fact that the overall accuracy takes into account both the accuracy of sensitive samples and normal samples. As the certified accuracy of sensitive samples increases, it dominates the overall accuracy and leads to its overall improvement.

Table 5 demonstrates the impact of different combinations of hyperparameters of (γ_1, γ_2) on both the overall accuracy and cost-sensitive performance. The choice of γ_1 and γ_2 is crucial and requires careful consideration. For γ_1 , setting a value that is too small can greatly undermine the overall accuracy, even though it may improve cost-sensitive robustness. This is because the performance of normal classes deteriorates, resulting in a degradation of overall performance. Otherwise, if the value is too large (i.e., $\gamma_1 = 8$), it has a negative impact on cost-sensitive performance.

Regarding γ_2 , it is evident that increasing its value while keeping γ_1 fixed leads to a significant improvement in cost-sensitive robustness. It is worth noting that even though the cost-sensitive seed class represents only a single seed, accounting for only 10% of the total classes, enhancing its robustness has a positive effect on overall accuracy as well. For instance, let’s compare the combination $(\gamma_1 = 4, \gamma_2 = 8)$ to $(\gamma_1 = 8, \gamma_2 = 8)$. We observe that the former, which exhibits better cost-sensitive robustness, outperforms the latter in terms of both overall accuracy and cost-sensitive robustness. It achieves an approximate improvement of 1.52% in overall accuracy and a significant improvement of approximately 50% in cost-sensitive robustness. This finding highlights the effectiveness of our subpopulation-based methods. It demonstrates that by fine-tuning the optimization thresholds for the certified radius of sensitive classes and normal classes separately, we can achieve a better trade-off between overall accuracy and cost-sensitive robustness.

Table 6: Certification results for various seedwise cost matrices with $\epsilon = 0.25$ and $\sigma = 0.25$ for both CIFAR-10 and Imagenette. Here, **Acc** stands for certified overall accuracy (%), **Rob_{c-s}** refers to certified cost-sensitive robustness (%).

Method	CIFAR-10				Imagenette			
	<i>S-Seed</i> (3)		<i>M-Seed</i> (2, 4)		<i>S-Seed</i> (7)		<i>M-Seed</i> (3, 7)	
	Acc	Rob _{c-s}	Acc	Rob _{c-s}	Acc	Rob _{c-s}	Acc	Rob _{c-s}
Gaussian	79.3	40.7	79.3	58.8	80.3	65.6	80.3	61.2
SmoothMix	73.0	32.6	73.0	46.4	81.4	61.9	81.4	59.2
SmoothAdv	77.9	42.8	77.9	52.5	77.8	66.6	77.8	59.3
MACER	80.8	47.5	80.8	65.3	79.6	70.1	79.6	66.2
Gaussian-R	77.8	58.3	78.4	63.5	73.8	74.2	76.4	65.6
SmoothMix-R	72.2	60.2	72.1	47.3	78.1	71.4	79.2	70.7
SmoothAdv-R	78.7	62.5	78.4	56.6	77.7	70.6	77.7	60.5
Ours	80.4	68.8	80.7	71.7	83.6	75.6	83.0	70.2

Table 7: Certification results for various pairwise cost matrices with $\epsilon = 0.25$ and $\sigma = 0.25$ for both CIFAR-10 and Imagenette. Here, **Acc** stands for certified overall accuracy (%), **Rob_{c-s}** refers to certified cost-sensitive robustness (%).

Method	CIFAR-10				Imagenette			
	<i>S-Pair</i> (3 → 5)		<i>M-Pair</i> (3 → 2, 4, 5)		<i>S-Pair</i> (7 → 2)		<i>M-Pair</i> (7 → 2, 4, 6)	
	Acc	Rob _{c-s}	Acc	Rob _{c-s}	Acc	Rob _{c-s}	Acc	Rob _{c-s}
Gaussian	79.3	67.4	79.3	51.5	80.3	88.0	80.3	73.0
SmoothMix	73.0	72.0	73.0	56.3	81.4	83.3	81.4	78.5
SmoothAdv	77.9	73.8	77.9	56.0	77.8	90.9	77.8	80.4
MACER	80.8	70.9	80.8	58.2	79.6	83.7	79.6	78.0
Gaussian-R	77.8	81.1	77.8	68.5	76.4	92.1	76.4	83.1
SmoothMix-R	72.2	75.7	72.2	73.8	78.1	84.8	78.1	81.8
SmoothAdv-R	78.7	77.4	78.1	66.3	77.7	91.8	77.6	82.0
Ours	80.9	93.5	80.7	91.4	83.6	94.2	83.2	84.2

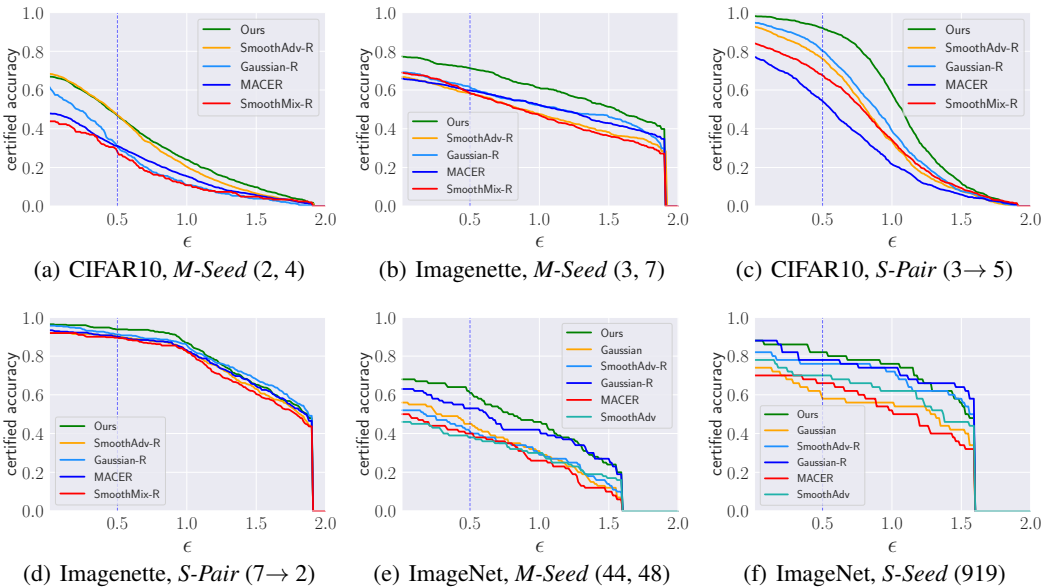


Figure 4: Certified accuracy curves for varying ϵ for different datasets and various cost matrix settings.

D.2 Certification Results with Varying Noises.

Results with Varying σ . We test the performance of our method under fixed ℓ_2 perturbations with $\epsilon = 0.25$ when the standard deviation parameter of the injected Gaussian noises is $\sigma = 0.25$. We demonstrate the results in Table 6 and Table 7 respectively for seedwise and pairwise cost matrices. The results show that our method consistently outperforms the several baseline randomized smoothing methods and their reweighting counterparts.

Results with Varying ϵ . We test the performance of our method under various ℓ_2 perturbations with different ϵ values and fix the standard deviation parameter of the injected Gaussian noises is $\sigma = 0.5$, same as in the Section 5. The results, shown in Figure 4 for both seedwise and pairwise cost matrices, demonstrate the superiority of our method compared to several baseline randomized smoothing methods and their reweighting counterparts. The corresponding settings are also reported in the main paper in Table 1, Table 2, and Table 3.

Table 8: Percentage for $\hat{r}_{\text{std}} > \hat{r}_{\text{c-s}}$ under different cost matrices settings same with Figure 2(c)-(d), we fix one seed class “cat” and vary the number of sensitive target classes in Ω_y .

$ \Omega_y $	1	3	5	7	9
Gaussian	0.9%	1.7%	13.7%	16.2%	22.1%
Ours	1.7%	6.8%	7.7%	10.8%	18.1%

Table 9: Avg. Seed represents the average results when selecting even classes (0, 2, 4, 6, 8) as sensitive seed classes. Avg. Target represents average results when fixing one sensitive seed class “cat” and varying the number of target classes in Ω_y where $|\Omega_y| = \{1, 3, 5, 7, 9\}$.

Method	Avg. Seed		Avg. Target	
	Acc	Rob _{c-s}	Acc	Rob _{c-s}
SmoothAdv-R	66.0 ± 0.6	54.2 ± 6.8	66.1 ± 0.4	61.7 ± 10.1
Ours	66.4 ± 0.7	62.8 ± 8.6	67.1 ± 3.2	74.7 ± 11.1

D.3 Additional Results

Comparing $\hat{r}_{\text{c-s}}$ with \hat{r}_{std} . Note that our proposed certification algorithm in Algorithm 1 returns the maximum of \hat{r}_{std} and $\hat{r}_{\text{c-s}}$ as the final certified radius. Here, we provide the concrete proportion for $\hat{r}_{\text{std}} > \hat{r}_{\text{c-s}}$ in Table 8 for different cost matrix settings to support our statement. Generally, when Ω_y contain the runner-up class and the condition for $\overline{p_B} = 1 - p_A$ holds, $\hat{r}_{\text{std}} > \hat{r}_{\text{c-s}}$; otherwise $\hat{r}_{\text{std}} < \hat{r}_{\text{c-s}}$. We give concrete examples for the two cases corresponding to settings in Table 8 when $|\Omega_y| = 9$, confirming the Rob_{c-s} measured by $\max(\hat{r}_{\text{c-s}}, \hat{r}_{\text{std}})$ is the possible tightest certificate:

- Case for $\hat{r}_{\text{std}} > \hat{r}_{\text{c-s}}$. The predicted probability is $[0.808, 0, 0.192, 0, 0, 0, 0, 0, 0]$, $\hat{r}_{\text{std}} = 0.429$ and $\hat{r}_{\text{c-s}} = 0.427$. we can observe the ground-truth class probabilities $h_\theta(\mathbf{x})$ not allocated to top class $g_\theta(\mathbf{x})$ to be entirely allocated to one runner-up class than to be allocated uniformly over all remaining classes. If this is the case, then setting $\overline{p_B} = 1 - p_A$ will yield a tight upper bound on p_B .
- Case for $\hat{r}_{\text{std}} < \hat{r}_{\text{c-s}}$. The predicted probability of sample \mathbf{x} belongs to class 3 is $[0.005, 0.000, 0.015, 0.836, 0.001, 0.071, 0.001, 0.068, 0.000, 0.003]$ where the top 1 class probability is 0.836, $\hat{r}_{\text{std}} = 0.481$ while $\hat{r}_{\text{c-s}} = 0.602$ correspondingly. On such case the class probabilities are allocated more uniformly across all remaining classes, $\overline{p_B} = 1 - p_A$ could be a loose upper bound of p_B , thus our $\hat{r}_{\text{c-s}}$ is better than \hat{r}_{std} for a tighter certificate.

Averaged Results. We also conduct experiments on average the results across multiple sensitive seed classes and multiple sensitive target classes for the CIFAR-10 dataset. We expect similar trends for other datasets. The results are reported in Table 9.

Heatmap Analysis. To further study the internal trade-off between our method and the fundamental baseline MACER, we present heatmaps of clean and robust test errors. It could be observed that compared with MACER, our method tends to let the predictions of all classes overfit on the sensitive seed class “cat”, misclassifications to other classes are reduced to a large extent, making the overall clean test error of our method less than that of MACER. For the sensitive seed class “cat”, we could observe its clean test error reduced from 40.1% to 11.1%, indicating our target cost-sensitive training method. Among the normal classes, our method has the most significant influence on is “dog”, increasing its misclassification rates to “cat” from 13.6% to 44.3%, decreasing its misclassification rates to other classes from 17.4% to 9.2%. In our *S-Seed* cost matrix settings, we do not need to care about one certain normal class’s misclassification rates as long as the overall misclassification rates are guaranteed, thus increasing the misclassification rates of class “dog” is tolerable in this case. The same trend is observed on the robust test error map, where the “cat” class’ robust test error decreases while the “dog” class’s robust test error increases. An interesting future work would be to design more balanced robust training methods.

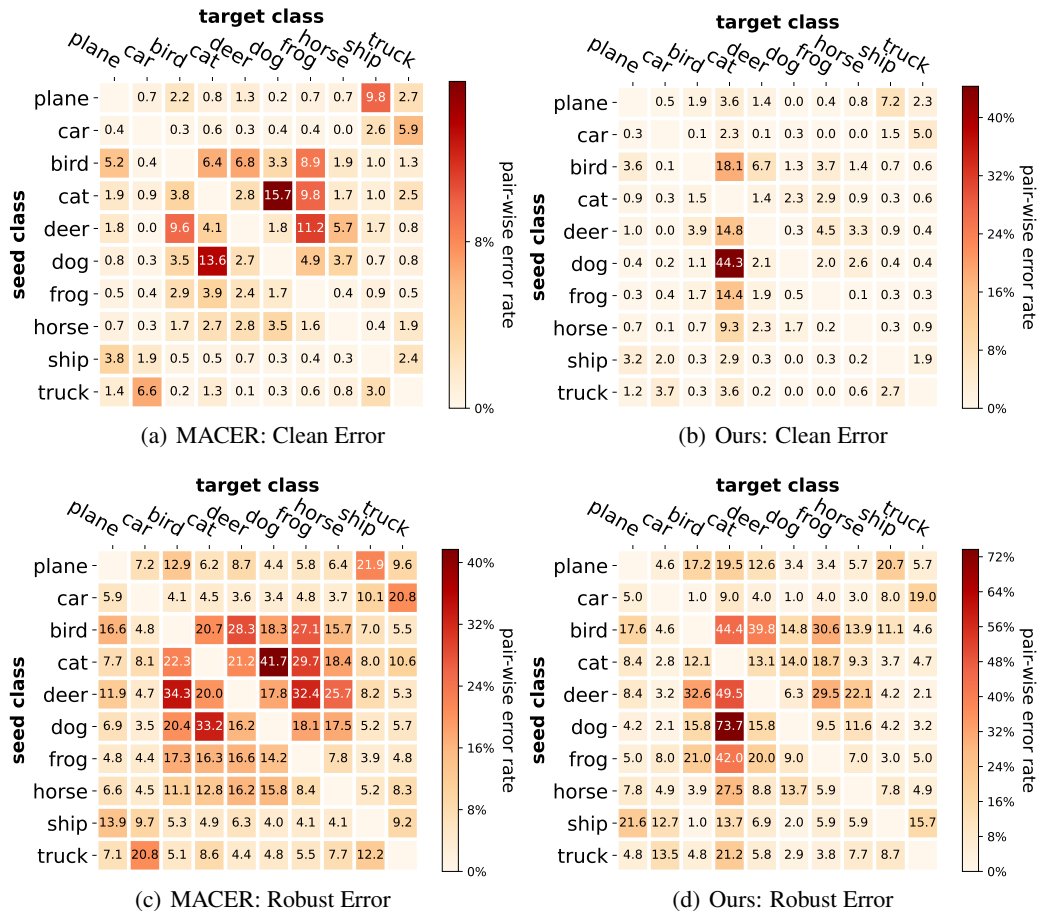


Figure 5: Figures (a) and (b): Heatmaps of clean test error on CIFAR-10 between MACER and ours. Figures (c) and (d): Heatmaps of robust test error on CIFAR-10 between MACER and ours. The cost-sensitive setting sets single seed “cat” as a sensitive seed class.